

PAPER • OPEN ACCESS

TiO₂ as conductivity enhancer in PVdF-HFP polymer electrolyte system

To cite this article: Shreya Bhattacharya *et al* 2017 *IOP Conf. Ser.: Mater. Sci. Eng.* **263** 022006

View the [article online](#) for updates and enhancements.

Related content

- [Improved properties of LiBOB-based solid polymer electrolyte by additive incorporation](#)
C Ratri, Q Sabrina, T Lestariningsih *et al.*
- [Developing dye sensitized solar cells with polymer electrolytes](#)
W Seesad, U Tipparach, N Kodtharin *et al.*
- [Effect of Poly\(Ether Urethane\) Introduction on the Performance of Polymer Electrolyte for All-Solid-State Dye-Sensitized Solar Cells](#)
Zhou Yan-Fang, Xiang Wan-Chun, Fang Shi-Bi *et al.*

TiO₂ as conductivity enhancer in PVdF-HFP polymer electrolyte system

Shreya Bhattacharya¹, Radha Manojkumar Ubarhande¹, M Usha Rani², Ravi Shanker Babu² and R Arunkumar¹

¹Department of Physics, School of Advanced Sciences, VIT University, Vellore, Tamil Nadu 632014, India

²Centre for Crystal Growth, VIT University, Vellore, Tamil Nadu, India

E-mail: usharani.m@vit.ac.in

Abstract. Composite polymer electrolytes were prepared by incorporating inorganic filler TiO₂ into PVdF-HFP-PMMA-EC-LiClO₄ system. The electrolyte films were prepared by solvent casting technique. The effect of inorganic filler on the conductivity of the blended polymer electrolyte was studied and it is found that there is a considerable increase in ionic conductivity $1.296 \times 10^{-3} \text{ S/cm}^{-1}$ on the addition of TiO₂. X-ray diffraction (XRD) study elucidate the increase in amorphous nature of the polymer electrolyte. This tendency of the polymer electrolyte could be the reason behind the increase in ionic conductivity. Fourier transform infrared spectroscopy (FTIR) spectra show the occurrence of complexation and interaction among the components.

1. Introduction

The idea of incorporating electrochemically inert particulate fillers into polymer matrices was introduced to enhance the mechanical stability in view of dimensionally stable polymer electrolytes for lithium batteries. The high surface area particulate fillers such as ZrO₂, TiO₂, Al₂O₃, hydrophobic fumed silica were incorporated into the polymer matrices to obtain the so called “composite polymer electrolytes”.

An increase in mechanical strength was observed in the composite electrolytes. Quite recently, composites based on gel electrolytes have also been prepared and improved room temperature conductivities were observed [1]. The addition of fine particles of Al₂O₃ to PEO-LiClO₄ complexed with dioctylphthalate exhibited an increase in conductivity by an order of magnitude. A noteworthy series of composite electrolytes based on PEO with the acronym ALPE (Advanced Lithium Polymer Electrolyte) membranes were prepared and the novelty of these electrolytes resides in their particular composition, which balances a combination of polymers, plasticizers, a selected lithium salt and a ceramic filler such as γ -LiAlO₂.

In addition to high ionic conductivities, the membranes are particularly characterized by a wide electrochemical stability window and stability towards the lithium metal. The improved stability of the lithium/electrolyte interface was attributed to the addition of dispersed γ -LiAlO₂ filler. The advantage of incorporating zeolite is two-fold. One is the enhancement in ionic conductivity at low temperatures.



Secondly, the addition of small amounts of inert filler particles will prevent this crystallization process, leading to the preservation of amorphous domains, which are responsible for ionic conduction.

The popular gel polymer electrolytes have high ionic conductivity, but the plasticizers employed in the electrolyte adversely reduce the mechanical strength of the polymer membrane and diminish its compatibility with lithium metal anode, leading to safety hazards [2]. On the other hand, addition of inorganic fillers such as, silica (SiO₂), copper oxide (CuO) and titania (TiO₂) nanoparticles to the polymer electrolyte results in the enhancement of physical strength as well as the increase in the absorption level of electrolytes solution [3-5]. Also, the inert fillers act as a solid plasticizer hindering the crystallization and reorganization of polymer chains by Lewis acid-base effect [6-10] so the properties such as ionic conductivity, lithium ions transference number, activation energy and stability at the interface with electrodes are improved.

The first such a system studied was LiI-Al₂O₃ and it was found that the conductivity was enhanced significantly with respect to LiI [11]. Further studies reveal, the composite polymer electrolytes alone can offer lithium polymer batteries with improved electrolyte/electrode compatibilities and safety hazards [12-15]. According to kumar et al. [16] the nanosized fillers are more compatible to reduce the interfacial resistance than fillers with micron sized.

In order to increase both the ionic conductivity and mechanical stability inorganic filler, nanosized TiO₂ is incorporated into preoptimized polymer blend electrolyte PVdFHFP-PMMA-EC-LiClO₄. The effect of the addition of TiO₂ (5, 10, 15 and 20 wt%) on the structural and ionic conductivity is discussed in detail.

2. Methodology

Poly(vinylidene fluoride-co-hexafluoropropylene) (PVdF-HFP) (average molecular weight 40 X 10⁴) and poly (methyl methacrylate) (PMMA) (average molecular weight 12 X10⁴) procured from Aldrich, USA were dried at 100°C under vacuum for 10 hr; LiClO₄ (Aldrich) was dried at 120°C under vacuum for 24 hr. Plasticizer ethylene carbonate (EC) (Aldrich) was used without further purification. Inert ceramic filler TiO₂ with particle size <100nm was purchased from Aldrich, USA and was used after annealing at 100°C for 10 hrs. The polymer electrolytes were prepared by solution casting technique. The preparation of composite polymer electrolytes involved the dispersion of the filler and the lithium salt in acetone followed by the addition of the polymer component. After the incorporation of the required components into the solution, the suspension was stirred for about 48 hr at room temperature and then at 60°C for 4 hr before the electrolyte was cast on finely-polished Teflon supports or Teflon covered glass plates. The films were dried in vacuum oven at 333K at a pressure of 10⁻³ torr for 24 hr. Further, the structural characters, complex formation and ionic conductivity (depend on temperature and inorganic filler) of the composite polymer electrolytes were confirmed by XRD (BRUKER x-ray diffractometer), FTIR (SHIMADZU IR AFFINITY spectrometer in the range of 4000 to 400 cm⁻¹) and ac impedance analysis (HIOKI 3532-50 LCR HiTESTER meter with frequency ranging from 50Hz to 5MHz) respectively.

3. Results and Discussion

3.1. Results of XRD Analysis.

X-ray diffraction patterns of PVdF-HFP, PMMA, LiClO₄, TiO₂ and the complexes are shown in Fig.3.1 (a & e-i), respectively. Crystalline peaks appearing at 18.4°, 20°, 26.7° and 38° (Fig. 3.1a) correspond to partial crystallization of PVdF units in the co-polymer giving a semi-crystalline structure of PVdF-HFP [17, 2]. The Amorphous nature of PMMA is evident from the absence of any sharp peak in Fig. 3.1 (b). The presence of diffraction peaks in Fig. 3.1 (c and d) indicates the crystalline nature of LiClO₄ & TiO₂, respectively. The complexes containing 0, 5, 10, 15 and 20 wt% of TiO₂ of the total polymer content of the electrolyte is depicted in Fig 3.1 (e-i). Intensity of the

diffraction peaks pertaining to PVdFHFP-PMMA-EC-LiClO₄ complex was found to decrease with increase of TiO₂ content. The diffraction peaks appearing at 18.4°, 20° pertaining to PVdF in PVdF-HFP disappears on addition of TiO₂. This result shows that the crystallinity of PVdF-HFP is reduced by the incorporation of TiO₂. This reduction in crystallinity upon the addition of TiO₂ is attributed to the chain re-organization and facilitates for higher ionic conduction. Some of the crystalline peaks corresponding to TiO₂ at 2θ values 38°, 70° and 75° are found absent in the complexes till the concentration of TiO₂ reaches 10 wt%, and above this concentration these peaks are found to reappear (Fig. 3 h & i) indicating excess TiO₂ in the polymer electrolyte. Some peaks (37°, 48°, 62°) are shifted in the complex indicating the interaction between the constituents of the complex.

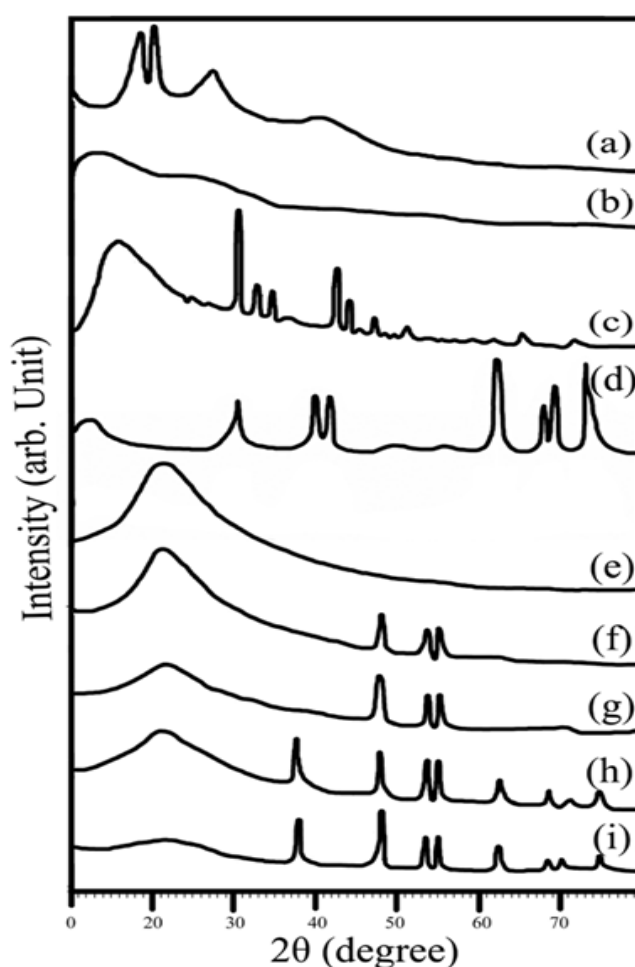


Figure 3.1 XRD patterns of pristine material (a)PVdF- HFP(b)PMMA (c) LiClO₄ (d) TiO₂ and (e-i) composite polymer electrolytes PVdF-HFP(17.25)-PMMA(5.75)-LiClO₄(8)-EC(69)-TiO₂(X) [X= 0 (e), 5 (f), 10 (g), 15 (h) and 20 (i)]

The crystalline peaks pertaining to TiO₂ are found to be minimal when the concentration is 10 wt% indicating the higher amorphous nature of the film (Fig.3.1g). The intensity of diffraction peaks obtained in the complexes increases with increase of TiO₂ content. It may be due to the phase separation of TiO₂ from the polymer complexes because the aggregated nano particles are not

consistent with the polymer matrix. This could be the reason for the lower conductivity of the film E₄ and E₅.

3.2. Results of FTIR characterization .

FTIR spectroscopy is important for the investigation of polymer structure. Since, it provides information about the complexation and interactions between the various constituents in the polymer electrolyte. These interactions can induce changes in the vibrational modes of the molecules in the polymer electrolyte. Fig. [3.2(a-e & f-j)] shows the FTIR spectra of pure PVdF-HFP, PMMA, LiClO₄, EC, TiO₂ and complexes respectively. The Fig. 3.2(a) shows that the group frequencies occurring at 1408 cm⁻¹, 1278 - 1179 cm⁻¹, 1065 cm⁻¹, 880 cm⁻¹, 510 cm⁻¹ and 488 cm⁻¹ correspond to -C-F stretching, -C-F & -CF₂- stretching, C-C skeletal vibration, Vinylidene group, CF₂ bending and CF₂ wagging of PVdF-HFP. The vibrational bands at 2952, 1733, 1437, 1388, 1242, 1195, 988, and 752 cm⁻¹ are assigned to CH₃ asymmetric stretching, C=O stretching vibration, O-CH₃ deformation, CH₃ symmetric bending, C-C-O vibrations, CH₂ twisting, CH₂ wagging, and CH₂ rocking vibrations of PMMA [Fig. 3.2(b)].

The strong vibrational bands at 530, 761 and 975 cm⁻¹ are characteristic peaks of α - phase PVdF crystals and the bands at 484 and 480 cm⁻¹ for PVdF γ and β phase, respectively [18]. It is evident from Fig. 3.2(f-j) that CH₃ asymmetrical stretching of PMMA is found to have shifted in all the complexes. The vibrational frequencies corresponding to carbonyl group C=O at 1733 cm⁻¹ of PMMA and 1867 cm⁻¹ of EC are found to be shifted to a common region around 1860 cm⁻¹ in all the complexes indicating the complex formation between the constituents.

Frequency band at 1485 cm⁻¹ attributed to CH₂ scissoring of PMMA is found to be shifted to a higher side in all the complexes. The band at 1451 cm⁻¹ representing O-CH₃ of PMMA and 1460 cm⁻¹ of PVdF-HFP are found to be absent in the complexes. Stretching frequency at 1399 cm⁻¹ representing -C-F of PVdF-HFP and CH₂ twisting of PMMA (1388 cm⁻¹) are absent in the complexes. Vibrational bands at 1278, 1179 cm⁻¹ of PVdF-HFP and 1242 cm⁻¹ of PMMA are found to be shifted to an intermediate region (1250 cm⁻¹) in all the complexes. CC skeletal breathing corresponding to PVdF-HFP is shifted around 1050 cm⁻¹ in all the complexes. C-H₂ wagging of PMMA is found to be shifted to 980, 976, 970 and 965 cm⁻¹ in the complexes containing 0, 5, 10, 15 wt% of TiO₂. The amorphous phase of PVdF-HFP at 879 cm⁻¹ is found to have an incremental shift (around 899 cm⁻¹) in complexes in accordance with the increase in TiO₂ content. The vibrational band at 839 cm⁻¹ is found to be shifted to a lower region in all the complexes. Furthermore CF₂ bending and CF₂ wagging of PVdF-HFP are found to be absent in all the complexes. The vibrational bands at 1072, 976, 763, 614 cm⁻¹ and bands at 879 and 841 cm⁻¹ are characteristic of the crystalline phase and amorphous phase of PVdF-HFP [19] respectively. These group frequencies are found to be shifted to the lower side indicating some alteration in their physical property of PVdF-HFP. The vibrational frequency at 1072 and 763 cm⁻¹ are missing in the complexes indicating the reduction in crystallinity and increase in amorphicity of the complexes. The peak intensities corresponding to partial crystallinity of polymer PVdF-HFP disappear with increase of TiO₂ content, except the vestige of vibrational frequency at 976 cm⁻¹ associated with the α - phase PVdF crystal even at higher concentrations of TiO₂ [20]. A new peak at around 3520 cm⁻¹ is found to be present in the entire complex except the one with the least content of TiO₂ [21,22] which could be due to the -OH stretching vibration band. This is in accordance with the results of Kim et al. [18]. From the above analysis, complex formation has been confirmed.

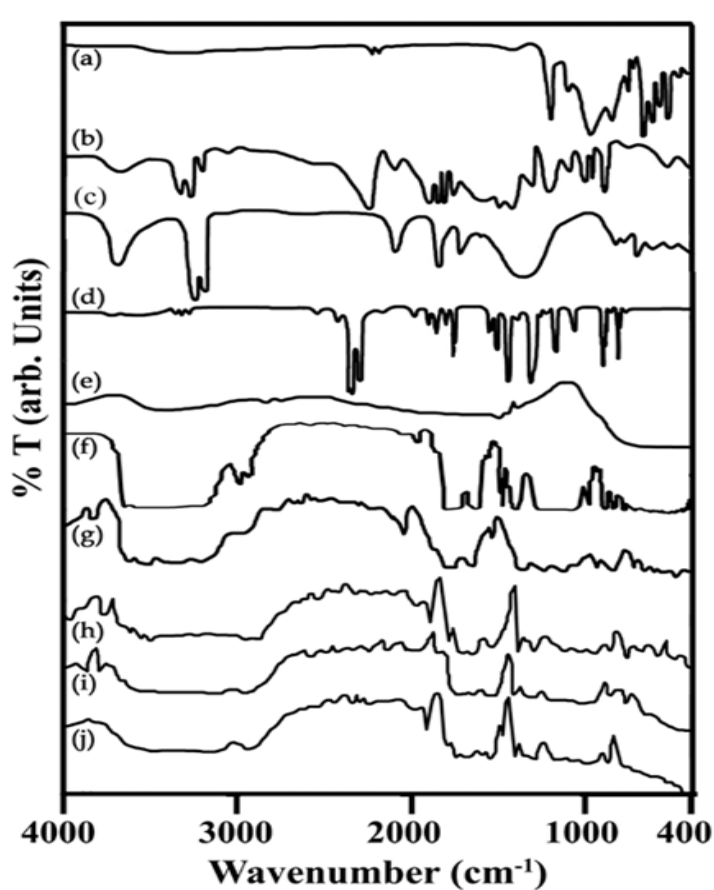


Figure 3.2 FTIR Spectra of pristine material (a)PVdF- HFP(b)PMMA (c) LiClO₄ (d) EC (e) TiO₂ and (f-j) composite polymer electrolytes PVdF-HFP(17.25) PMMA(5.75)–LiClO₄(8)-EC(69)-TiO₂(X) [X= 0 (f), 5 (g), 10 (h), 15 (i) and 20 (j)]

3.3 Results of conductivity studies.

The ionic conductivity of composite polymer electrolytes is given in Table 3.1. Figures 3.3, 3.4 and 3.5 depict the temperature dependent ionic conductivity, cole-cole plots of impedance and dependence of conductivity with ceramic content. The disappearance of the semicircular portion at high frequencies in the complex impedance plot asserts the total conductivity is the result of ion conduction [23]. At low frequency, the complex impedance plot must show a straight line parallel to the imaginary axis, but the double layer at the blocking electrodes causes the curvature [24].

It is clear from the figure that the ionic conductivity has considerably increased upon the addition of inert filler. The ionic conductivity of the inert filler system is higher than the undoped system for all the temperatures studied. The ionic conductivity increases with the increase of filler content upto 10% and decreases even when the concentration of filler was increased. These results are in accordance with those reported earlier in which Al₂O₃ was used as filler in PEO-based electrolytes [25]. As commonly found in composite materials, the conductivity is not linear function of the filler

concentration. At low concentration levels the diffusion effect which, tends to depress the conductivity, is effectively contrasted by the specific interaction of the ceramic surfaces, which promotes fast ion transport and follows the Arrhenius conductivity. Hence, an apparent enhancement in conductivity is seen at lower concentration.

At higher concentration of ceramic additives, the dilution effect predominates and the conductivity is lowered [26]. According to Scrosati et. al. [27] from their NMR studies that the local dynamics of the lithium ions, in particular lithium mobility, is not changed by filler which supports the idea that the enhancement of conductivity by adding filler is caused by stabilizing and increasing the fraction of amorphous phase. The XRD results obtained by our studies also substantiate it. It is evident from table 3.1 that the film E₃ with 10% of TiO₂ shows highest ionic conductivity. Apart from the above said reason the increase in conductivity can be attributed to (i) the ceramic particles acting as nucleation centers for the formation of minute crystallites [27-29]; (ii) the ceramic particles aiding in the formation of amorphous phase in the polymer electrolyte [30-32]; (iii) to the formation of the new kinetic path via polymer-ceramic boundaries [33-35]. Irrespective of the reasoning, it can safely be assumed that as the T_g decreases, the amorphous phase or the less ordered regions become more flexible resulting in increased segmental motion of the polymer chains as reflected by enhanced conductivity [36]. The decrease in ionic conductivity after optimum concentration of TiO₂ could be asserted due to the building up of continuous non conductive phase by large amount of fillers acting as an electrically inert component would block up lithium ion transport, resulting in increase in total resistance of the composite polymer electrolyte. It is reported, for many composite polymer electrolytes formed by the addition of filler that, ionic conductivity increases to reach its maximum value at 5-10 wt% of filler [38].

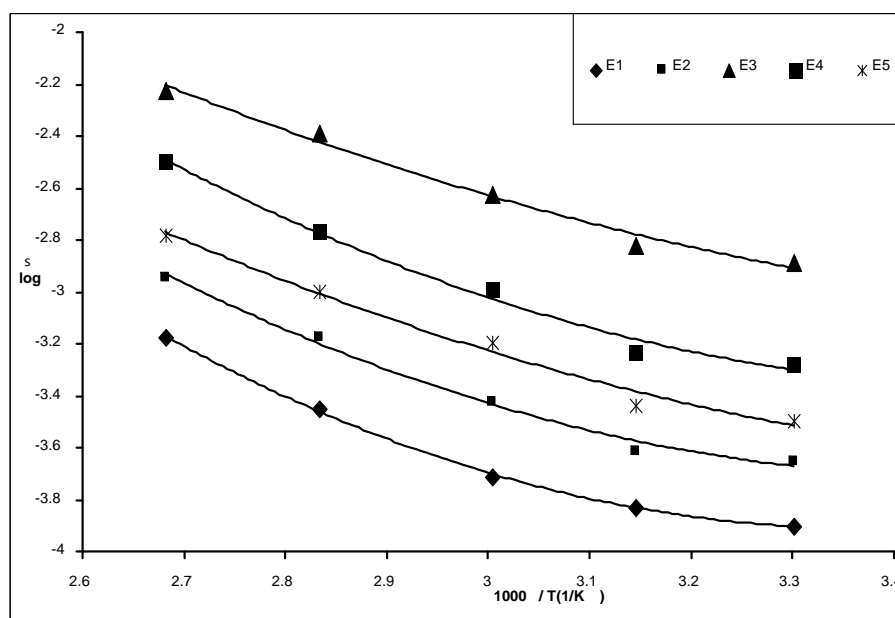


Figure 3.3 Arrhenius plot of the conductivity for PVdF-HFP-PMMA-LiClO₄-EC polymer complexes for TiO₂ (0,5,10,15,20 wt%) concentrations.

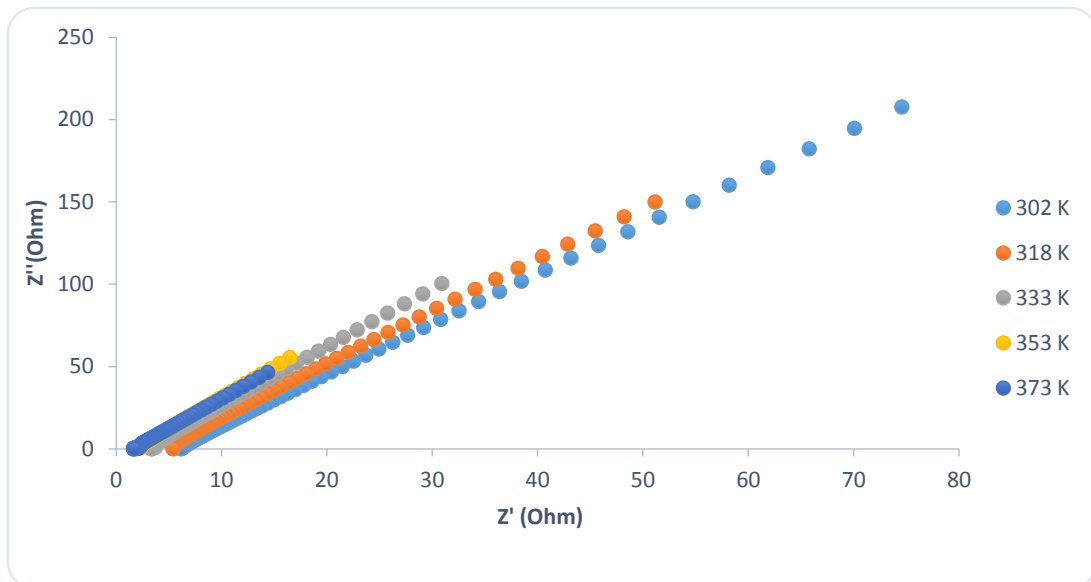


Figure 3.4 Impedance diagram for PVdF-HFP(17.25)-PMMA(5.75)-LiClO₄(8)-EC(69)-TiO₂(10) at different temperatures

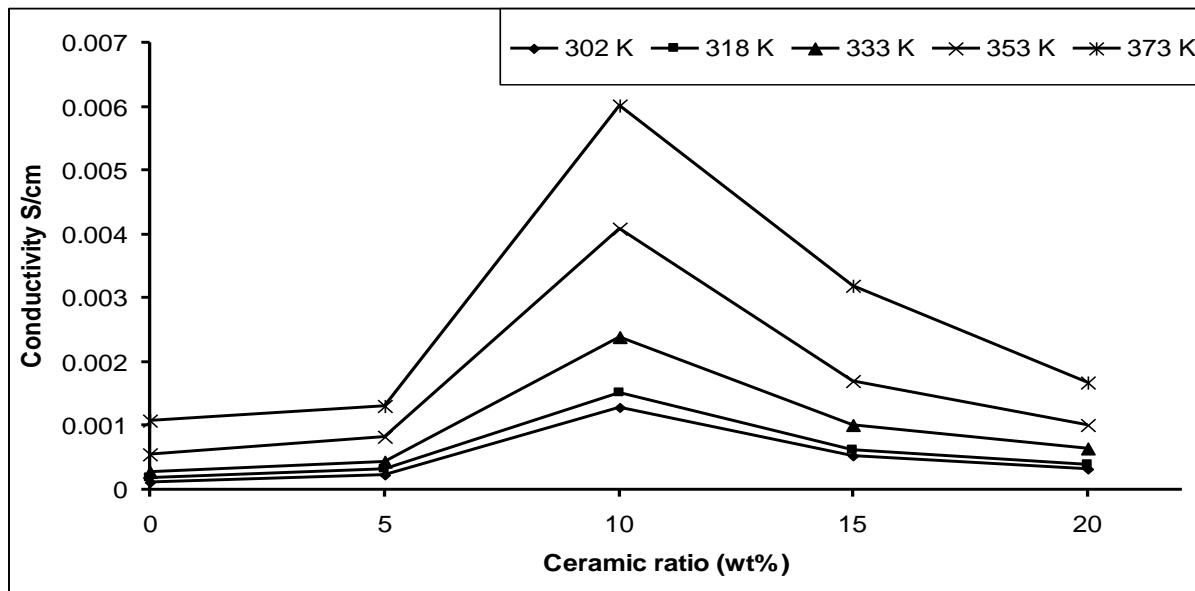


Figure 3.5 Variation of ionic conductivity with TiO₂ concentrations.

Sample	Concentration PVdF-HFP - PMMA- LiClO ₄ -EC- TiO ₂ (0,5,10,15,20 wt%)	Conductivity σ ($\times 10^{-3}$ S cm ⁻¹)				
		302 K	318 K	333 K	353 K	373 K
E ₁	17.25-5.75-8-69-0	0.125	0.184	0.282	0.546	1.084
E ₂	17.25-5.75-8-69-5	0.222	0.310	0.443	0.816	1.303
E ₃	17.25-5.75-8-69-10	1.296	1.510	2.384	4.085	6.011
E ₄	17.25-5.75-8-69-15	0.525	0.620	1.021	1.698	3.191
E ₅	17.25-5.75-8-69-20	0.320	0.390	0.638	1.00	1.67

Table 3.1 Conductivity values of PVdF-HFP- PMMA- LiClO₄ - EC with TiO₂ (0, 5, 10, 15, 20 wt%)

Conclusion

The composite polymer electrolytes (PVdF-HFP(17.25)-PMMA(5.75)- LiClO₄(8)- EC(69)) filled with different amounts of TiO₂ nanoparticles have been prepared by solvent casting technique. The crystallinity of polymer matrix decreases with the increase of wt% of TiO₂ due to their solid plasticization effect. The complex formation, and structural behaviours have been confirmed by FTIR, XRD studies. It is observed that PVdF-HFP (17.25) - PMMA (5.75) - LiClO₄ (8) - EC (69) - TiO₂ (10wt%) complex gives appreciable conductivity (1.296×10^{-3} Scm⁻¹).

References

- [1] A. Manuel Stephan, *Eur. Polym. J.* **42** (2006) 21.
- [2] J. J. Song, Y. Y. Wang, C.C. Wan, *J. Power Sources* **77** (1999) 183.
- [3] K. M. Kim, K. S. Ryu, S.-G. Kang, S.H. Chang, *Polymer* **43** (2002) 3951.
- [4] M. Caillon – Caravanier, B. Claude – Montigny, D. Lemordant, G. Bossier, *J. Power Sources* **107** (2002) 125.
- [5] B. Wang, L. Gu, *Mater. Lett.* **57** (2002) 361.
- [6] W. Wiczonek, K. Such, J.R. Steven, *Electrochim. Acta* **40** (1995) 2251.
- [7] B. Kumar, S.J. Rodrigues, S. Kota, *Electrochim. Acta* **47** (2002) 4125.
- [8] F. Croce, L. Persi, B. Scrosati, F. Serraino- Fiory, E. Plichta, M.A. Hendrickson, *Electrochim. Acta* **46** (2001) 2457.
- [9] W. Wiczonek, P. Lipka, G. Zukowska, H. Wycislik, *J. Phys. Chem., B* **102** (1998) 6968.
- [10] P. P. Prosini, P. Villano, M. Carawska, *Electrochim. Acta* **48** (2003) 272.
- [11] C. C. Liang, *J. Electrochem. Soc.* **120** (1973) 1289.
- [12] G.B. Appetecchi, J. Hassoun, B. Scrosati, F. Croce, F. Cassel, M. Salomon, *J. Power Sources*, **124** (2003) 246.
- [13] F. Croce, L. Persi, B. Scrosati, F. Serraino- Fiory, E. Plichta, M.A. Hendrickson, *Electrochim. Acta* **46** (2001) 2457.
- [14] R.G. Singhal, M.D. Capracotta, J.D. Martin, S.A. Khan, P.S. Fedkiw, *J. Power Sources*, **128** (2004) 247.

- [15] M. Morita, T. Fujisaki, N. Yoshimoto, M. Ishikawa, *Electrochim. Acta* **46** (2001) 1565.
- [16] B. Kumar, *J. Power Sources*, **135** (2004) 215.
- [17] C. Leonard, J.L. Halary, L. Monnerie, *Polymer* **26** (1985) 1507.
- [18] K.M. Kim, J.M. Ko, N.G. Park, K.S. Ryu, S.H. Chang, *Solid State Ionics* **161** (2003) 121.
- [19] Z. Li, G. Su, X. Wang, D. Gao, *Solid State Ionics* **176** (2005) 1903.
- [20] K.M. Kim, N.-G. Park, K.S. Ryu, S.H. Chang, *Polymer* **43** (2002) 3951.
- [21] P. Jones, J.A. Hockey, *Trans. Faraday Soc.*, **67** (1971) 2669.
- [22] T. Ivanova, A. Harizanova, *Solid State Ionics* **138** (2001) 227.
- [23] M.M.E. Jacob, S.R.S. Prabaharan, S. Radhakrishnan, *Solid State Ionics* **104**, (1997) 105.
- [24] C. Kim, G. Lee, K. Lio, K.S. Ryu, S.G. Kang, S.H. Chang, *Solid State Ionics* **123** (1999) 251.
- [25] X. Qian, N. Gu, Z. Cheng, X. Yang, E. Wang, S. Dong, *Electrochim. Acta.* **46** (2001) 1829.
- [26] F. Croce, L. Persi, B. Scrosati, F. Serraino-Fiory, E. Plichta, M.A. Hendrikson, *Electrochim. Acta* **46** (2001) 2457.
- [27] J. Plocharsi, W. Wieczorek, *Solid State Ionics* **28** (1988) 979.
- [28] W. Weiczorek, *Mater. Sci. Eng. B* **15** (1992) 108.
- [29] A. Chandra, P. C. Srivastava, S. Chandra, *J. Mater. Sci.* **30** (1995) 3633.
- [30] J. Przulski, K. Such, H. Wycishik, *Synth. Met.* **35** (1990) 241.
- [31] J. Plocharski, W. Weiczorek, J. Przulski, K. Such. *Appl. Phys., A* **49** (1989) 55.
- [32] M. Munichandraiah, L. G. Scanlon, R. A. Marsh, B. Kumar, A. K. Sircar, *J. Appl. Electrochem.* **25** (1995) 857.
- [33] B. Kumar, L. G. Scanlon, *J. Power Sources* **52** (1994) 261.
- [34] M. Munichandraiah, L. G. Scanlon, R. A. Marsh, B. Kumar, A. K. Sircar, *J. Appl. Electrochem.* **24** (1994) 1066.
- [35] J. Przulski, M. Sickierski, W. Wieczorek, *Electrochim Acta* **40** (1995) 2101.
- [36] B. K. Choi, Y. W. Kim, K. H. Shiv, *J. Power sources* **68** (1997) 357.
- [37] Z. Wen, T. Itoh, M. Ikeda, N. Hirata, M. Kubo, O. Yamamoto, *J. Power Sources* **90** (2000) 20.
- [38] B. Scrosati, F. Croce, *Poly. Adv. Technol.* **4** (1993) 198.